STAT4, a potential predictor of prognosis, promotes CD8 T-cell infiltration in ovarian serous carcinoma by inducing CCL5 secretion

WEI WANG[1,2*], SI LIU[1,2*], FUNIAN LU[1,2], BIN YANG[1,2], XUCUI ZHUANG[1,2], JINGJING YIN[1,2], GANG CHEN[1,2] and CHAOYANG SUN[1,2]

[1]Department of Obstetrics and Gynecology, Tongji Hospital, Tongji Medical College, Huazhong University of Science and Technology, Wuhan, Hubei 430030; [2]National Clinical Research Center for Obstetrics and Gynecology, Cancer Biology Research Center (Key Laboratory of The Ministry of Education), Tongji Hospital, Tongji Medical College, Huazhong University of Science and Technology, Wuhan, Hubei 430110, P.R. China

Received October 27, 2022; Accepted April 20, 2023

DOI: 10.3892/or.2023.8577

Abstract. Ovarian serous carcinoma (OC) is a common cause of mortality among gynecological malignancies. Although tumor-infiltrating CD8 T cells are associated with a favorable prognosis of OC, the underlying mechanisms are not clearly understood. The present study identified the key genes and potential molecular mechanisms associated with CD8 T-cell infiltration in OC. The score of CD8 T cells in The Cancer Genome Atlas dataset (376 samples from patients with OC) was estimated using the quanTIseq and MCP-counter algorithms. Thereafter, a protein-protein interaction network of differentially expressed genes was constructed and the hub genes were identified using cytoHubba in Cytoscape. The results revealed that signal transducer and activator of transcription 4 (*STAT4*) was strongly correlated with CD8 T-cell infiltration in OC. Furthermore, the prognostic value of *STAT4* in OC was verified by Kaplan-Meier curve, and univariate and multivariate analyses. The biological functions of *STAT4* were determined by Gene Ontology and Kyoto Encyclopedia of Genes and Genomes pathway analyses, which revealed that *STAT4* is closely related to cytokines in OC. Moreover, Spearman correlation analysis suggested that *STAT4* was most positively correlated with CC chemokine ligand 5 (*CCL5*). CCL5 was revealed to be critical for orchestrating T-cell infiltration in tumors. Moreover, immunohistochemistry and reverse transcription-quantitative PCR showed that STAT4, CCL5 and CD8A (a marker for CD8 T cells) were closely related in OC. Moreover, *in vitro* analysis revealed that *STAT4* knockdown led to a decrease in CCL5 expression and CD8 T-cell migration. Taken together, the present study suggested that *STAT4* may regulate CD8 T-cell infiltration in OC tissues by inducing CCL5 secretion. Furthermore, *STAT4* may be considered a promising prognostic biomarker for OC.

Correspondence to: Professor Chaoyang Sun, Department of Obstetrics and Gynecology, Tongji Hospital, Tongji Medical College, Huazhong University of Science and Technology, 1095 Jiefang Avenue, Wuhan, Hubei 430030, P.R. China
E-mail: suncydoctor@gmail.com

*Contributed equally

Abbreviations: OC, ovarian serous carcinoma; TCGA, The Cancer Genome Atlas; DEGs, differentially expressed genes; PPI, protein-protein interaction; TILs, tumor-infiltrating lymphocytes; STAT4, signal transducer and activator of transcription 4; GEO, Gene Expression Omnibus; GO, Gene Ontology; KEGG, Kyoto Encyclopedia of Genes and Genomes; GSEA, Gene Set Enrichment Analysis; IHC, immunohistochemistry; OS, overall survival; DSS, disease-specific survival; DFI, disease-free interval; PFI, progression-free interval; HR, hazard ratio; CI, confidence interval

Key words: CD8 T cell, STAT4, CCL5, OC, prognosis

Introduction

Ovarian cancer is a deadly gynecological cancer, with a 5-year survival rate of 30-40% in the United States (1,2). Ovarian serous carcinoma (OC) is the most common histological subtype of ovarian cancer and accounts for 70-80% of ovarian cancer-related deaths (3,4). Immunotherapy, an emerging field in tumor treatment, has achieved therapeutic effects only in a small subset of patients with ovarian cancer (5,6). Moreover, a previous study reported that immunotherapy has better therapeutic efficacy in patients with a pre-existing T-cell response against the tumor (7). However, although T-cell infiltration exhibits a significant effect *in situ*, it is detected in only ~50% of ovarian cancer tissues at diagnosis (8). CD8 T cells are major immune mediators of tumor rejection, and it has been reported that CD8 tumor-infiltrating lymphocytes (TILs) are associated with a favorable prognosis in OC (9). Therefore, it is important to investigate the mechanisms of CD8 T-cell infiltration in OC, to identify new diagnostic biomarkers for OC.

Signal transducer and activator of transcription 4 (STAT4) is a key mediator of pro-inflammatory immune responses and affects several immune cells by mediating interleukin (IL)-12

signaling (10). For example, STAT4 mediates the induction of interferon-γ production in CD4, CD8, natural killer cells and macrophages (11,12), and stimulates the development of fully functional Th1 cells (13). Considering its important immune modulatory function, the role of STAT4 has also been studied extensively in carcinogenesis. Previous studies have indicated that high STAT4 expression is a prognostic factor for survival in breast carcinoma, hepatic carcinoma and ovarian cancer (14-16).

Chemokines serve an important role in regulating tumor immune cell infiltration. Previous studies have suggested that the expression of several chemokines, including CC chemokine ligand (CCL)2, CCL3, CCL4, CCL5, chemokine C-X-C ligand (CXCL)9 and CXCL10, is associated with TIL recruitment in melanoma (17,18). For example, CCL4 has been shown to have a key role in recruiting BATF3-expressing dendritic cells (DCs), which affects T-cell inflammation in melanoma (18,19). In addition, tumors, such as ovarian cancer, express multiple chemokines, which permit the infiltration of peripheral blood CD4 and CD8 T cells to the ovarian cancer site (20). Moreover, tumor cell-expressed CCL5, and macrophage and DC-expressed CXCL9 have been shown to promote T-cell infiltration at the ovarian cancer site (21).

The present study aimed to identify the potential biomarkers affecting CD8 TILs and their role in OC prognosis, and to further explore the underlying mechanisms.

Materials and methods

Clinical specimens and ethics statement. Tissues were obtained from 25 patients with OC (age, 40-70 years; mean age, 53.6 years) between January and December 2020 from the Department of Obstetrics and Gynecology, Tongji Hospital, Tongji Medical College (Wuhan, China). Patients who did not provide consent were excluded. A total of 25˚C tissues were collected by surgery for immunohistochemical staining, whereas 16 surgically removed fresh OC tissues were frozen and stored at -80˚C for western blotting and reverse transcription-quantitative PCR (RT-qPCR). Peripheral blood was obtained from three healthy female donors (age, 20-40 years; mean age, 33.7 years) with an unremarkable medical history between May 2 and May 5, 2021. The collection and use of human samples in the present study was approved by the Ethics Committee of Tongji Hospital (approval no. TJ-IRB20190320).

Data acquisition. RNA-sequencing (RNA-seq) data were obtained from TCGA-ovarian serous cystadenocarcinoma (OV) dataset (376 samples from patients with OC; https://portal.gdc.cancer.gov/repository) and clinical data were obtained from TCGA pan-cancer clinical data resource, a standardized dataset developed by Liu *et al* (22). However, due to a lack of data regarding disease-free interval (DFI; the time to recurrence from first diagnosis) and/or progression-free interval (PFI; the period from the date of diagnosis until the date of the first occurrence of a new tumor event) for all patients, the numbers of patients with DFI and/or PFI data were less than the numbers of patients with overall survival (OS; the date of diagnosis to the date of death from any cause), disease-specific survival (DSS; defined as death from the diagnosed cancer type; Liu *et al* combined the fields of 'tumor_status' with 'vital status' to derive a surrogate for DSS, by approximating 'Dead' and 'With Tumor' as a DSS event) data. The microarray data were obtained from the GSE53963 (https://www.ncbi.nlm.nih.gov/geo/query/acc.cgi?acc=GSE53963) (23), GSE32062 (https://www.ncbi.nlm.nih.gov/geo/query/acc.cgi?acc=GSE32062) (24) and GSE130571 (https://www.ncbi.nlm.nih.gov/geo/query/acc.cgi?acc=GSE130571) (21) datasets from the GEO database.

Differentially expressed gene (DEG) analysis. Gene expression values from TCGA-OV database were expressed as transcripts per million. The RNA-seq data corresponding to recurrent tumors, based on TCGA-OV annotation, were excluded from the present study for the following reasons. Firstly, a comparison of primary and relapsed tumors has shown that specific molecular alterations can appear in the relapsed tumors (25,26). Moreover, Sun *et al* (27) found a significant difference in the immune microenvironments of recurrent and primary hepatocellular carcinoma cases, suggesting that the immune microenvironment may also differ between primary and recurrent tumors in OC. Secondly, since TCGA database focuses on primary tumors, there were only a few recurrent tumor samples (n=5) to conduct a reliable analysis. Subsequently, quanTIseq and MCP-counter in R script were used to quantify the relative proportions of infiltrating CD8 T cells (28,29). Thereafter, the optimal cutoff point (0.3) was determined using the R package 'survminer' (https://cran.r-project.org/package=survminer) and all of the patients were classified into CD8 T cell high- and low-score groups, based on this cutoff value. The DEGs in the high- and low-score groups were determined using DESeq2 (https://bioconductor.org/packages/release/bioc/html/DESeq2.html) at |log2 fold change|>1 and Benjamini-Hochberg-adjusted P<0.05.

Construction of a protein-protein interaction (PPI) network and identification of hub genes. The Search Tool for the Retrieval of Interacting Genes/Proteins (STRING) database was used to build a PPI network of DEGs (30) and a confidence score of ≥0.4 was used as the cutoff standard. To identify specific functional genes, the top 90 overlapping genes were screened using 12 different methods, Maximal Clique Centrality, Density of Maximum Neighborhood Component, Maximum Neighborhood Component, Edge Percolated Component, Degree, Stress, BottleNeck, Closeness, EcCentricity, Radiality, Betweenness and ClusteringCoefficient, based on the Cytoscape plug-in cytoHubba (https://apps.cytoscape.org/apps/cytohubba).

Functional enrichment analysis. Gene Ontology Biological Process (GOBP) term and Kyoto Encyclopedia of Genes and Genomes (KEGG) pathway analyses were conducted using the 'clusterProfiler' package (31). The false discovery rate <0.05 was set as the cut-off value. Gene Set Enrichment Analysis (GSEA) was performed to further determine the KEGG pathways and GOBP terms that were correlated with *STAT4* expression. The genes were ranked according to their Spearman correlation with *STAT4* expression levels, and the genes with an absolute value of correlation coefficients |rhol>0.3 and P<0.05 were selected.

Immunohistochemistry (IHC). The OC tissues were fixed in 4% paraformaldehyde for 24 h at room temperature, embedded in paraffin, and cut into 4-μm sections for immunohistochemical analysis using rabbit/mouse streptavidin-peroxidase kits (cat. nos. SP-9001/SP-9002; OriGene Technologies, Inc.) according to the manufacturer's instructions. Antigen retrieval was performed with EDTA buffer (pH 9) at 95˚C for 10 min, after which, the sections were washed with PBS followed by the addition of 3% H_2O_2 at 37˚C for 30 min to remove endogenous peroxidase. After sufficient washing with PBS, the sections were incubated with 5% BSA (cat. no. G5001; Wuhan Servicebio Technology Co., Ltd) for 30 min at 37˚C. Subsequently, the sectioned tissues were incubated with primary antibody at 4˚C overnight. The following antibodies were used: CD8A (1:2,000; cat. no. ab245118; Abcam), STAT4 (1:200; cat. no. 13028-1-AP; Proteintech Group, Inc.) and CCL5 (1:50; cat. no. A5630; Abclonal Biotech Co., Ltd.). Staining was visualized using DAB (cat. no. ZLI-9019; OriGene Technologies, Inc.) and counterstaining was performed with hematoxylin for 1 min at room temperature. The staining was captured under a light microscope (Olympus Corporation). For STAT4 and CCL5, the histochemistry score (H-Score) was calculated as follows: H-Score=(% cells of weak intensity x1) + (% cells of moderate intensity x2) + (% cells of strong intensity x3) (32). For CD8A, the number of positive cells was counted in five random fields of view under a x20 magnification to calculate the mean number of positive cells.

Cell culture and transfection. The OVCAR8, HOC7, SKOV3 and CAOV3 (serous adenocarcinoma) human ovarian cancer cell lines were obtained from the American Type Culture Collection. OVCAR8 cells were cultured in RPMI-1640 (cat. no. 11875119; Gibco; Thermo Fisher Scientific, Inc.) supplemented with 10% FBS (cat. no. 16140089; Gibco; Thermo Fisher Scientific, Inc.), HOC7 cells were cultured in DMEM (cat. no. 11965092; Gibco; Thermo Fisher Scientific, Inc.) supplemented with 10% FBS, SKOV3 cells were cultured in McCoy's 5A (cat. no. 16600082; Gibco; Thermo Fisher Scientific, Inc.) supplemented with 10% FBS, and CAOV3 cells were cultured in RPMI-1640 supplemented with 20% FBS. All cells were maintained in a humidified atmosphere containing 5% CO_2 at 37˚C. OVCAR8 and CAOV3 cells were seeded in six-well plates at a density of 60-70% confluence, then transfected with control small interfering RNA (siRNA) (non-targeting sequence: 5'-TTCTCCGAACGTGTCACGT-3'), human *STAT4* siRNA_1 (targeting sequence: 5'-GCCTGACCATAGATTTGGA-3') or human *STAT4* siRNA_2 (targeting sequence: 5'-AACGGCTGTTGCTAAAGGA-3') (all 50 nM; Guangzhou RiboBio Co., Ltd.) using Lipofectamine® 3000 reagent (Invitrogen; Thermo Fisher Scientific, Inc.) according to the manufacturer's instructions. After 24 h, the medium was replaced with fresh culture medium and to the cells were cultured for another 48 h in a humidified atmosphere containing 5% CO_2 at 37˚C. The cells were then collected and knockdown efficiency was verified using western blot analysis and RT-qPCR.

RNA isolation and RT-qPCR. Total RNA was extracted from OC tissues or cells using the Total RNA kit (cat. no. RC101; Vazyme Biotech Co., Ltd.) according to the manufacturer's instructions. For all samples, RNA was then reverse transcribed into cDNA using HiScript II Q RT SuperMix (cat. no. R223-01; Vazyme Biotech Co., Ltd.) according to the manufacturer's protocol. Subsequently, cDNA levels were quantified using SYBR Green qPCR (cat. no. Q711; Vazyme Biotech Co., Ltd.) in triplicate. Each sample was amplified and normalized to the housekeeping gene GAPDH, and the relative fold change of mRNA expression was measured using the $2^{-\Delta\Delta Cq}$ method (33). The primer sequences were as follows: Human CD8A, forward 5'-TCCATCATGTACTTCAGCCACTT-3' and reverse 5'-GGTGATAACCAGTGACAGGAGAA-3'; human STAT4, forward 5'-CTCAGAGGCCGTTGGTACTTAAA-3' and reverse 5'-TCCTTTGGTTGCAAATGTCGAAAT-3'; human CCL5, forward 5'-CGTGCCCACATCAAGGAGTATTT-3' and reverse 5'-TTGATGTACTCCCGAACCCATTT-3'; and human GAPDH, forward 5'-GGAGTCCACTGGCGTCTTCA-3' and reverse 5'-GTCATGAGTCCTTCCACGATACC-3'. qPCR was performed using a qPCR instrument (Bio-Rad Laboratories, Inc.) and the cycling conditions were as follows: 3 min at 95˚C for polymerase activation, followed by 45 cycles at 95˚C for 15 sec, 60˚C for 30 sec and 72˚C for 30 sec, and fluorescence collection at 95˚C for 15 sec.

Western blot analysis. Total proteins were extracted from cells and tissues using the ExKine Total Protein Extraction Kit (cat. no. KTP3006; Abbkine Scientific Co., Ltd.) and the extracted proteins were quantified using the BCA protein analysis kit (cat. no. G2026-200T; Wuhan Servicebio Technology Co., Ltd.) according to the manufacturer's protocol. Equal amounts of protein (20 μg) from each sample were loaded into each lane and separated by SDS-PAGE on a 10% gel. Subsequently, proteins were transferred to PDVF membranes. After being blocked with 5% BSA, the membranes were incubated with specific antibodies overnight. The following primary antibodies were used: CD8A (1:5,000; cat. no. 66868-1-lg; Proteintech Group, Inc.), STAT4 (1:600; cat. no. 13028-1-AP; Proteintech Group, Inc.), CCL5 (1:1,000; cat. no. A5630; Abclonal Biotech Co., Ltd.), GAPDH (1:50,000; cat. no. 60004-1-Ig; Proteintech Group, Inc.) and β-actin (1:50,000; cat. no. 81115-1-RR; Proteintech Group, Inc.). The membranes were then incubated with HRP-conjugated goat anti-rabbit IgG/anti-mouse IgG (1:5,000; cat. no. Ant020/Ant019; Antgene) for 1 h at room temperature. Finally, blots were visualized using the western blotting detection kit WesternBright ECL (cat. no. K-12045-D50; Advansta, Inc.). GAPDH and β-actin were used as loading controls. Protein semi-quantification was performed using ImageJ software (v1.49p; National Institutes of Health).

ELISA. Cell supernatants were collected 48 h after transfection, and CCL5 levels were measured using a CCL5 ELISA kit (cat. no. RK00077; Abclonal Biotech Co., Ltd.), according to the manufacturer's instructions. The results were obtained using a microplate reader (Bio-Rad Laboratories, Inc.) set to 450 nm, and the readings were corrected at 570 nm. Since the ELISA kit was designed for serum, plasma and cell culture supernatant samples, the components of a more complex ovarian cancer homogenate may interfere with CCL5 quantification by ELISA. For example, matrix components often interfere with sample analysis and affect the accuracy of the

results (34). Therefore, to detect CCL5 content, ELISA was used for cellular experiments and western blot analysis was used for fresh-frozen tissue samples.

Chemotaxis assay. To assess lymphocyte migration, peripheral blood lymphocytes were isolated from healthy donors by gradient centrifugation (1,000 x g for 20 min) at room temperature, then stimulated with 5 μg/ml anti-CD3 (cat. no. BE0001-2; Bio X Cell) and anti-CD28 (cat. no. 40-0289; Cytek Biosciences) for 2 days at 37˚C, after which, the cells were cultured in the presence of 20 ng/ml recombinant human IL-2 (cat. no. 200-02; PeproTech, Inc.) for 5 days at 37˚C. Thereafter, 80,000 lymphocytes were resuspended in 150 μl RPMI-1640 and placed in the top well of a Transwell migration chamber (pore size, 5 μm; Corning, Inc.). CAOV3 cells transfected with control siRNA or human *STAT4* siRNA were seeded 24 h earlier in the bottom well of the Transwell migration chamber. CD8 T cells that migrated to the bottom chamber were evaluated after 24 h by flow cytometry. The cells in the bottom chamber were collected, washed with PBS and then incubated with allophycocyanin-conjugated anti-human CD8A antibodies (5 μl/test; cat. no. 300911; BioLegend, Inc.) on ice for 20 min. The samples were collected and analyzed by flow cytometry (FACSCalibur; BD Biosciences) and CytExpert (v2.4.0.28; Beckman Coulter, Inc.) were used for data analyses. I results were expressed as chemotactic index, which was defined as the ratio of cell migration towards the medium of cells transfected with human *STAT4* siRNA compared with control siRNA.

Statistical analysis. In the present study, the optimal cutoff values of CD8 T cells or gene expression were determined using the R package 'survminer' based on the correlation with patient survival. Survival analysis by Kaplan-Meier was performed using survminer R packages and the P-value of each Kaplan Meier-plot was calculated by log-rank test. Individuals with <30 days follow-up were excluded to remove the potential bias associated with treatment effects, as a short follow-up period can lead to an overestimation of OS/progression-free survival (35). Survival analysis was also carried out on the Kaplan-Meier plotter website (https://kmplot.com). Cox univariate and multivariate regression analyses were conducted to evaluate the effects of variables on survival. Unpaired Student's t-test was used for comparisons between two groups, whereas one-way ANOVA with Tukey's post hoc test was used for comparisons between multiple groups. Correlation coefficients were evaluated by Spearman analyses. The R package ggplot2 (https://ggplot2.tidyverse.org/) was used to map the relationship between *STAT4* and chemokine genes expression levels. All statistical analyses were conducted using GraphPad Prism software (v8.3.0; Dotmatics) or R software (v4.0.3; https://www.r-project.org/). All experiments were carried out in triplicate and data are expressed as the mean ± SD. $P<0.05$ was considered to indicate a statistically significant difference.

Results

Association of CD8 TILs with survival in patients with OC. The present study evaluated the immune populations in TCGA-OV dataset using both quanTIseq and MCP-counter algorithms to enhance accuracy. The quanTIseq algorithm predicted the composition of 10 immune cell types in OC tissues, whereas the MCP-counter algorithm quantified the abundance of eight immune cell types and two stromal cell types (cancer associated fibroblasts and endothelial cell) in OC tissues (Fig. S1A and B). Thereafter, all of the patients were classified into high- and low-score groups based on the average CD8 T-cell infiltration score (cutoff values: quanTIseq, 0.0027; MCP-counter, 0.3526). Survival time data were obtained from TCGA pan-cancer clinical data resource (22) and Kaplan-Meier survival curve analysis was used to evaluate the prognostic impact of CD8 T-cell infiltration in OC. Consistent with the previous analysis (9), the results revealed that high CD8 T-cell scores were significantly associated with a better prognosis of patients with OC (Fig. 1A and B).

Identification of CD8 T-cell infiltration-related genes in OC. Patients were classified into high and low CD8 T-cell score groups according to the results of the quanTIseq and MCP-counter algorithms. Subsequently, differential gene expression analysis was performed to identify DEGs between the high and low CD8 T-cell score groups. There were 665 significantly upregulated genes and 104 significantly downregulated genes in the high CD8 T-cell score group identified by the quanTIseq algorithm. Similarly, 651 genes were upregulated and 67 genes were downregulated according to the MCP-counter algorithm (Fig. 2A). The overlapping genes (551 upregulated and 29 downregulated) in the two groups were selected as candidate genes for further analysis (Fig. 2B). To determine the association between the candidate DEGs and CD8 T-cell infiltration in OC, a PPI network was constructed with 228 nodes (223 upregulated and five downregulated nodes) using the STRING database and it was visualized using Cytoscape (Fig. 2C). Finally, the GOBP enrichment analysis of the 228 nodes was conducted to determine their associated molecular mechanisms. As shown in Fig. 2D, these nodes were found to be primarily associated with 'T cell activation', which is consistent with the biological role of CD8 TILs.

STAT4 is a potential marker of CD8 T-cell infiltration in OC. The top 90 overlapping hub genes in the PPI network were first analyzed using twelve algorithms from the CytoHubba plug-in, after which a flower plot was created to determine significant hub genes shared across all of the groups; ultimately, a list of five genes was identified (Fig. 3A). To further determine the relationship between these five genes and CD8 T-cell infiltration, the Spearman correlation coefficients between their gene expression values and CD8 T-cell scores were calculated, and three key genes (*CD5*, *SLAMF1* and *STAT4*) with a Spearman correlation coefficient ≥0.5 were identified (Fig. 3B). Previous studies have reported that *CD5* and *SLAMF1* are widely expressed on cells within the hematopoietic system and are closely associated with T-cell activation (36-38); therefore, these were not pursued further in the present study. Whereas *STAT4* was highly correlated with CD8 T-cell infiltration and has rarely been reported to be involved in tumor immune cell infiltration (39). Analysis of TCGA-OV database revealed that *CD8A* expression was significantly correlated with CD8 T-cell infiltration level (Fig. S2) and thus may be used as a marker gene for quantifying CD8 TILs (21). In addition, the results confirmed the positive correlation between *CD8A* and *STAT4*

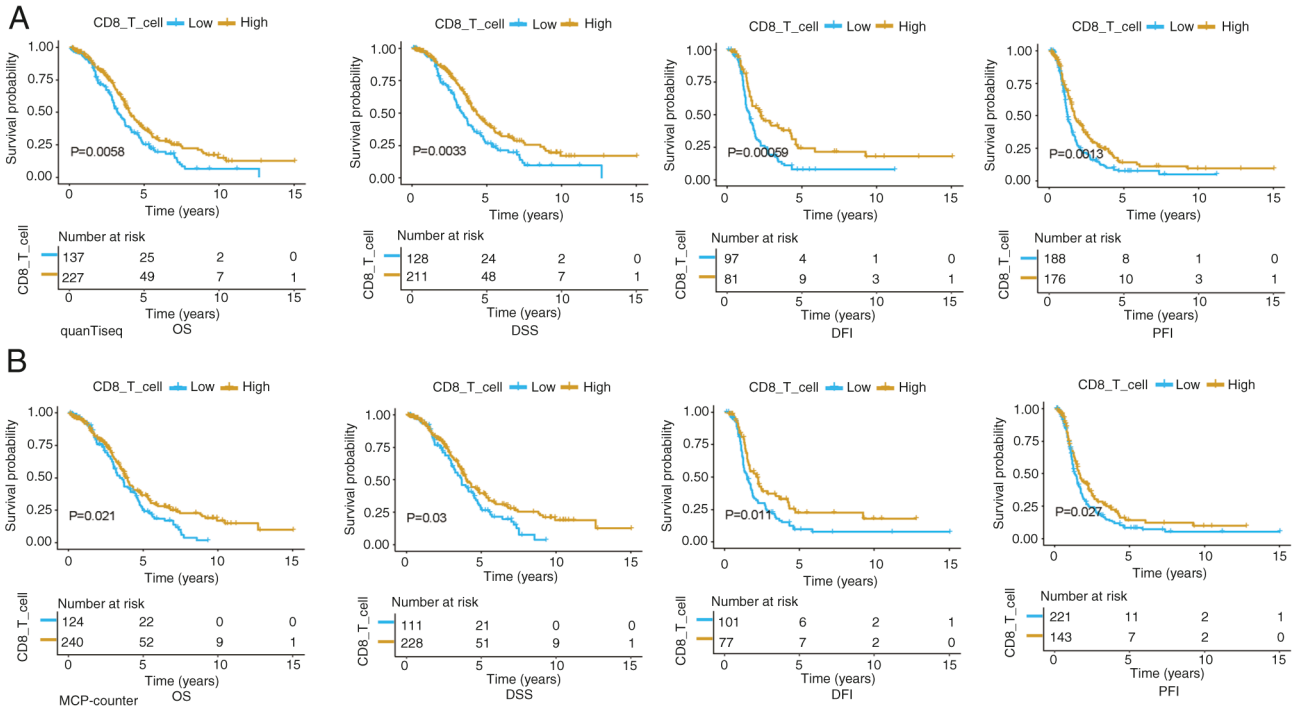

Figure 1. CD8 T-cell score is significantly related to the prognosis of patients with OC. Based on the CD8 T-cell score, patients with OC were divided into high/low score groups. (A) Kaplan-Meier curve of the high and low CD8 T-cell score groups quantified by the quanTIseq algorithm. (B) Kaplan-Meier curve of the high and low CD8 T-cell score groups quantified by the MCP-counter algorithm. P-values were calculated by log-rank test. OC, ovarian serous carcinoma; OS, overall survival; DSS, disease-specific survival; DFI, disease-free interval; PFI, progression-free interval.

expression in an independent set of 16 OC specimens using RT-qPCR analysis (Fig. 3C). Moreover, similar results were obtained in the xenografts of the mouse ovarian cancer cell line ID8 (GSE130571); *STAT4* expression was significantly increased in tumors with CD8 T-cell infiltration compared with in those lacking CD8 TILs (Fig. 3D). The present study further assessed the association of *STAT4* expression levels with age and the clinical stage of OC, and revealed that age was not associated with *STAT4* expression levels (Fig. S3A); however, *STAT4* expression was elevated in early-stage patients (I/II) compared with in advanced-stage patients (III/IV), although the difference was not statistically significant (Fig. S3B). This was possibly because the majority of the samples were obtained from the patients with advanced stage OC (>94%). Subsequent Kaplan-Meier survival curves of Kaplan-Meier plotter database, TCGA, GSE53963 and GSE32062 datasets revealed that patients with high *STAT4* expression had a significantly better prognosis than those with low *STAT4* expression in patients with OC (Fig. 3E-H). Similar findings were observed in the univariate Cox regression analysis and *STAT4* expression was significantly associated with survival in TCGA and GSE32062. Multivariate Cox regression analysis of TCGA, GSE53963 and GSE32062 data [hazard ratio=0.74, 0.57 and 0.8; 95% confidence interval=0.55-0.99, 0.26-1.2 and 0.68-0.95; P=0.044, 0.149 and 0.01, respectively; Fig. 3I) revealed that high *STAT4* expression may serve as an independent biomarker for a favorable prognosis. Therefore, *STAT4* was chosen as the candidate gene for further analyses.

STAT4 is strongly associated with CCL5 in OC. KEGG and GO analyses were performed to determine the biological functions of the *STAT4*-associated genes in OC. Firstly, TCGA, GSE53963 and GSE32062 datasets were screened to obtain 2,100, 1,907 and 2,197 *STAT4*-associated genes, respectively (|rho|>0.3 and P<0.05). GOBP analysis revealed that these *STAT4*-associated genes were mostly involved in 'leukocyte-mediated immunity' and 'positive regulation of cytokine production'. The KEGG pathway analysis revealed that these genes were associated with 'cytokine-cytokine receptor interaction' and 'chemokine signaling pathway' (Fig. 4A). Furthermore, GSEA demonstrated a clear positive correlation between *STAT4* expression and the aforementioned processes (Fig. S4A-D). These findings suggested that *STAT4* may be involved in the production of cytokines, especially chemokines. Therefore, the present study further assessed the relationship between *STAT4* and chemokines, and revealed that *STAT4* was positively correlated with chemokines in all three datasets. Notably, these data all showed that *STAT4* was most significantly correlated with *CCL5* (Fig. 4B). Further RT-qPCR analysis of *CCL5* and *STAT4* in an independent set of 16 OC specimens revealed a positive correlation between the two genes (Fig. 4C). Similarly, a positive correlation was also observed in the ID8 tumor tissues (GSE130571) (Fig. 4D). Moreover, the expression of *STAT4* was significantly higher in tumors with CD8 T-cell infiltration compared with in those lacking CD8 T cells (Fig. 4E).

STAT4, CCL5 and CD8 T-cell infiltration are closely associated in OC. Dangaj *et al* (21) reported that CD8 T-cell infiltration required tumor cell-derived CCL5. Consistently, the present study observed that *CCL5* expression was significantly positively correlated with CD8 T-cell infiltration level in TCGA-OV dataset (Fig. S5A and B). Similar results were

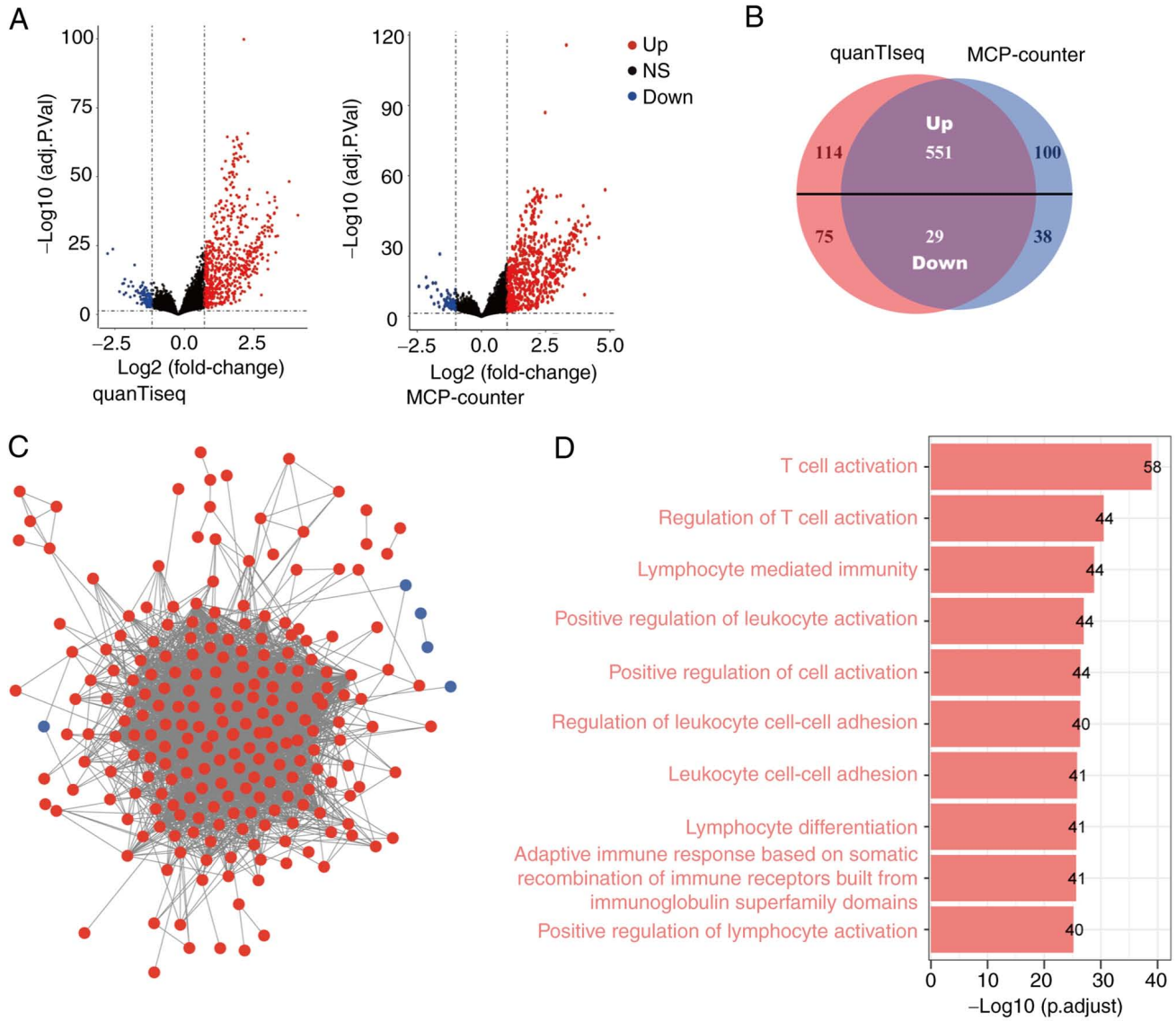

Figure 2. Comparison of gene expression profiles based on CD8 T-cell score and the PPI network in OC. (A) Volcano map of DEGs according to the CD8 T-cell score quantified by the quanTIseq (left panel) and MCP-counter (right panel) algorithms. P-values were calculated using the DESeq2 package and were corrected by Benjamini-Hochberg adjustment. (B) Venn diagram analysis of DEGs according to the CD8 T-cell scores quantified by the quanTIseq and MCP-counter algorithms. (C) PPI network constructed by Search Tool for the Retrieval of Interacting Genes/Proteins (confidence score, 0.4) and visualized by Cytoscape. Red nodes represent upregulated DEGs, blue nodes represent downregulated DEGs. (D) Results of Gene Ontology Biological Process enrichment analysis of nodes. Numbers in the bars indicate the number of genes. DEGs, differentially expressed genes; NS, not significant; PPI, protein-protein interaction.

also observed between *CD8A* and *CCL5* by RT-qPCR analysis of 16 OC specimens (Fig. S5C). Furthermore, western blot analysis revealed that the protein expression levels of STAT4, CCL5 and CD8A in OC specimens were positively correlated with each other (Fig. 5A and B). In addition, IHC analysis of STAT4, CCL5 and CD8A in OC specimens revealed that STAT4 and CCL5 were highly expressed in OC tissues, and that STAT4 was significantly correlated with CD8A and CCL5. Additionally, there was a correlation between CD8A and CCL5, although not statistically significant (Fig. 5C and D). Based on these results, we hypothesized that STAT4 may influence CD8 T-cell infiltration in OC by regulating CCL5 expression.

STAT4 promotes CD8 T-cell migration by inducing CCL5 secretion. To confirm whether STAT4 induces CCL5 secretion, the expression levels of *STAT4* and *CCL5* were examined in four ovarian cancer cell lines (HOC7, SKOV3, CAOV3 and OVCAR8). The results revealed that the expression levels of *STAT4* were low in the HOC7 cell line, but high in SKOV3, OVCAR8 and CAOV3 cell lines, especially in the SKOV3 cell line. Additionally, the expression levels of CCL5 were low in the HOC7 and SKOV3 cell lines, but were higher in the OVCAR8 and CAOV3 cell lines, with the highest expression in the CAOV3 cell line (Fig. S6A-C). Therefore, CAOV3 and OVCAR8 cell lines were selected for *STAT4* gene knockdown analyses. As shown in Fig. 6A and B, STAT4 was significantly downregulated at both the mRNA and protein levels in CAOV3 cell line transfected with the indicated siRNAs, indicating successful knockdown of the *STAT4* gene. Subsequent analysis of *CCL5* expression revealed that *STAT4* knockdown significantly suppressed *CCL5* expression in the CAOV3 cell

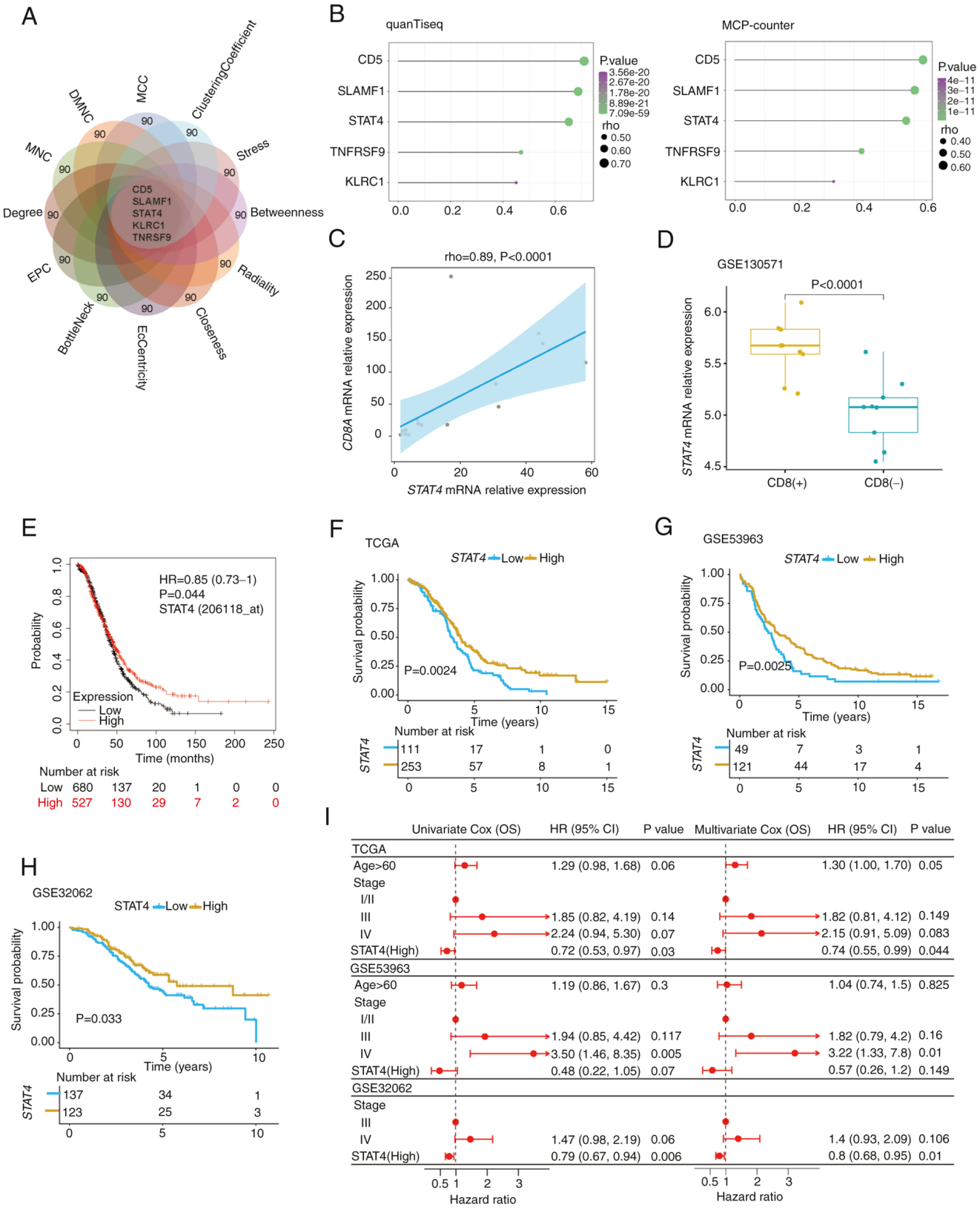

Figure 3. *STAT4* expression is correlated with CD8 T-cell infiltration level. (A) Flower plot displaying the genes shared between the twelve different methods based on the Cytoscape plug-in cytoHubba. The number of top hub genes and the corresponding method in cytoHubba are indicated on each petal. (B) mRNA expression of the shared genes was positively correlated with CD8 T-cell infiltration level in TCGA-OV quantified by the quanTIseq or MCP-counter algorithms. (C) Spearman correlation plots of *STAT4* with *CD8A* quantified by reverse transcription-quantitative PCR in an independent set of 16 ovarian serous carcinoma specimens. Correlation coefficients (rho) and P-values (Spearman rank test) are displayed. (D) mRNA expression levels of *STAT4* were analyzed in ID8 tumors lacking CD8 TILs [CD8(-)] and tumors infiltrated with CD8 T cells [CD8(+)] (GSE130571). Unpaired t-test was performed. Kaplan-Meier curves of the OS between low- and high *STAT4* expression groups in (E) Kaplan-Meier plotter database, (F) TCGA-OV, (G) GSE53963 and (H) GSE32062 cohorts. P-values were calculated by log-rank test. (I) Univariate and multivariate Cox regression analyses of *STAT4* level, age and tumor stage in TCGA-OV, GSE53963 and GSE32062 cohorts. HR and P-values are displayed. TCGA-OV, The Cancer Genome Atlas-ovarian serous cystadenocarcinoma; OS, overall survival; HR, hazard ratio; CI, confidence interval; STAT4, signal transducer and activator of transcription 4.

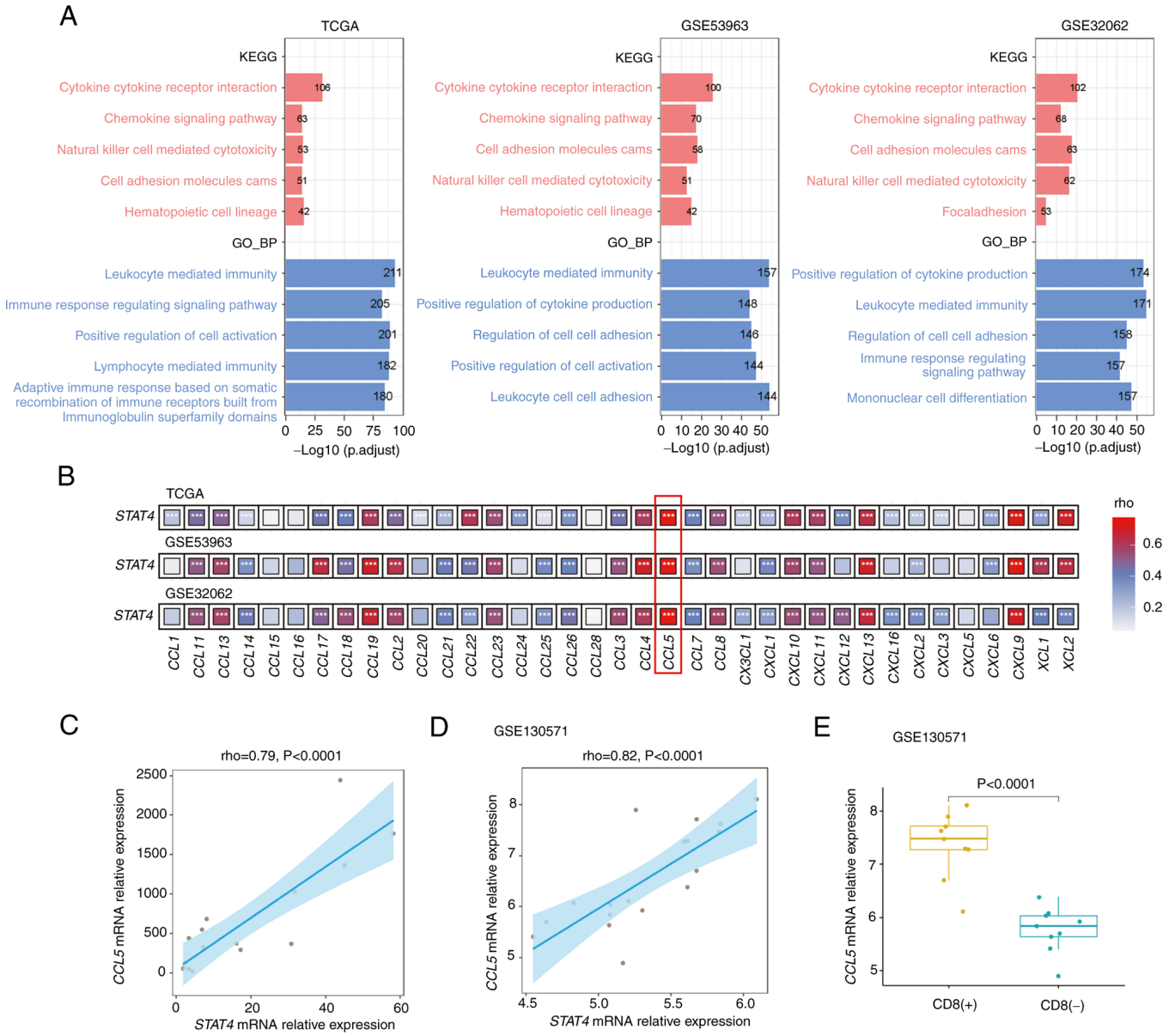

Figure 4. *STAT4* is strongly associated with chemokines in OC. (A) KEGG pathway analysis showed that *STAT4* was mostly associated with 'cytokine-cytokine receptor interaction' and 'chemokine signaling pathway' in TCGA, GSE53963 and GSE32062 datasets (upper panel). GOBP analysis showed *STAT4* was mostly involved in the; positive regulation of cytokine production' (lower panel). (B) Heatmap represents the correlation between *STAT4* expression and chemokine genes. ***P≤0.001, Spearman rank test was performed. (C) Spearman correlation plots of *STAT4* with *CCL5* quantified by reverse transcription-quantitative PCR in an independent set of 16 OC specimens. Correlation coefficients (rho) and P-values (Spearman rank test) are displayed. (D) Spearman correlation plots of *STAT4* with *CCL5* mRNA levels in the GSE130571 dataset. (E) mRNA expression levels of *CCL5* were analyzed in tumors with CD8 T-cell infiltration [CD8(+)] and that lacking CD8 T cells [CD8(-)]. Unpaired t-test was performed. OC, ovarian serous carcinoma; KEGG, Kyoto Encyclopedia of Genes and Genomes; TCGA, The Cancer Genome Atlas; GO BP, Gene Ontology Biological Process; STAT4, signal transducer and activator of transcription 4; CCL5, CC chemokine ligand 5.

line and cell culture supernatant (Fig. 6C and D). By contrast, although the mRNA expression levels of *STAT4* were also significantly downregulated in the OVCAR8 cell line, the silencing effect was relatively weak. Additionally, knockdown of *STAT4* resulted in a non-significant decrease in the expression levels of CCL5 (Fig. S6D-G), which may be due to the relatively low *STAT4* expression in the OVCAR8 cell line, resulting in insignificant changes in CCL5. Subsequently, it was determined whether *STAT4* affected CD8 T-cell migration by performing a chemotaxis assay of autologous blood T cells; the results revealed that the recruitment of CD8 T cells to cancer cells was attenuated by *STAT4* knockdown (Fig. 6E-G). Therefore, these results validated the hypothesis that *STAT4* promotes CD8 T-cell migration by inducing CCL5 secretion.

Discussion

CD8 T cells serve a crucial role in antitumor immune responses (40). It has been reported that CD8 T-cell infiltration is associated with a better prognosis in OC (9); however, an Italian study showed that T-cell infiltration was detected in only ~50% of ovarian cancer tissues (8). Moreover, the mechanism of CD8 T-cell infiltration in OC is poorly understood. The transcriptome represents tumor heterogeneity, and to gain

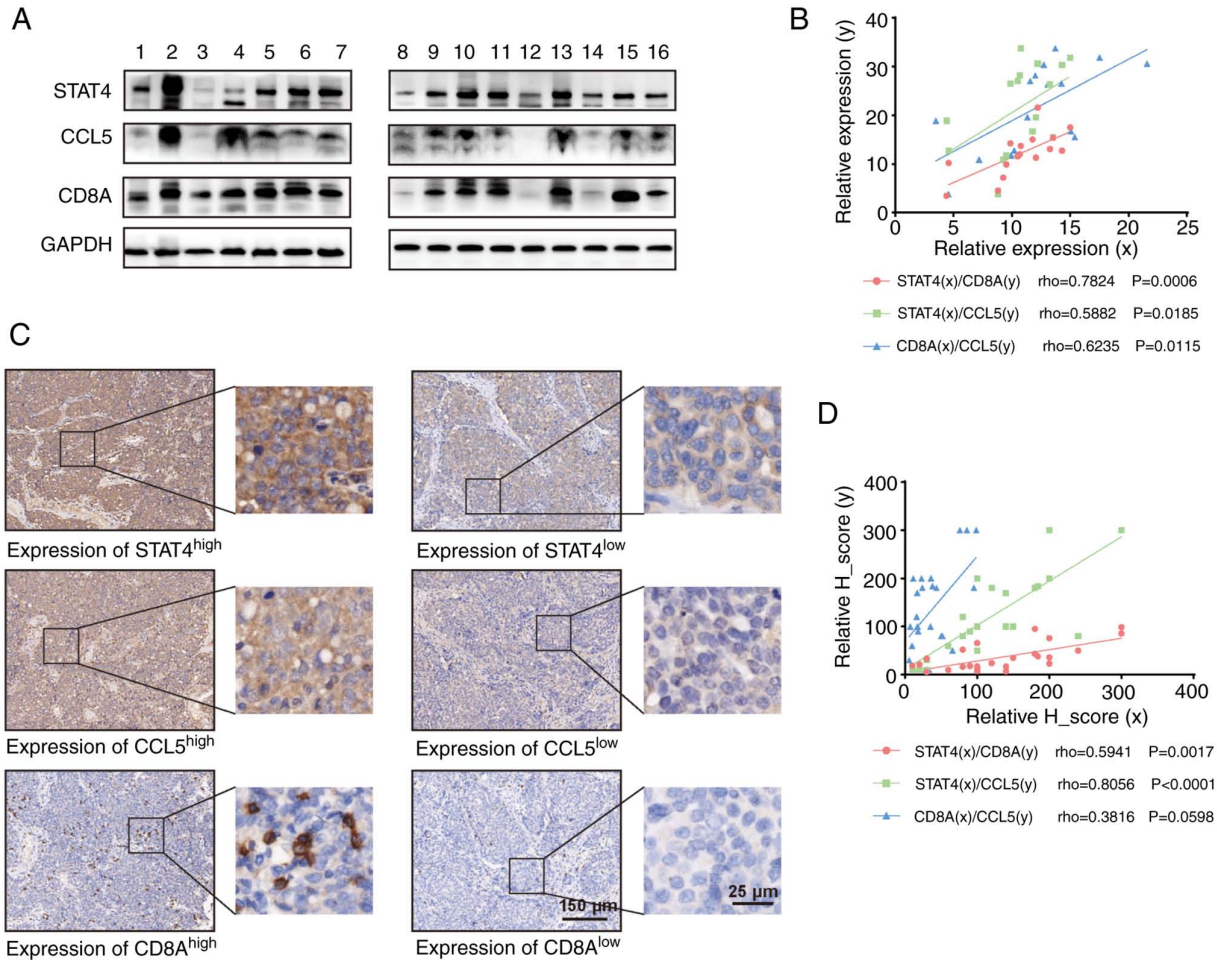

Figure 5. STAT4 and CCL5 expression, and CD8 T-cell infiltration in OC are intercorrelated. (A) Western blot analysis of STAT4, CCL5 and CD8A in 16 OC tissues. GAPDH or β-actin were used as a loading control. (B) Semi-quantification of western blotting showed that STAT4, CCL5 and CD8A were positively correlated. (C) Representative immunostaining for the indicated proteins (STAT4, CCL5 and CD8A) in OC tissue. (D) Semi-quantification of STAT4, CCL5 and CD8A immunohistochemistry staining (n=25) showed that STAT4, CCL5 and CD8A were positively correlated. Spearman rank test was performed. OC, ovarian serous carcinoma; STAT4, signal transducer and activator of transcription 4; CCL5, CC chemokine ligand 5.

insights into the mechanism of CD8 T-cell infiltration in OC, the present study screened TCGA and GEO datasets for CD8 T-cell infiltration-related biomarkers through the quanTIseq and MCP-counter algorithms.

The R scripts, including CIBERSORT-CBS, CIBERSORT-CBA, EPIC, MCP-counter, quanTIseq, TIMER and xCell, which are used to quantify infiltrating immune cells conceptually fall into two categories, marker gene-based or deconvolution-based. Sturm *et al* (41) demonstrated that quanTIseq gave the most accurate estimates of CD8 T cells (r=0.98; P<0.001) among the deconvolution-based R scripts, whereas MCP-counter gave the most accurate estimates of CD8 T cells (r=0.95; P<0.001) among the marker gene-based R scripts. Therefore, the present study first estimated the CD8 T-cell score in TCGA-OV dataset using the quanTIseq and MCP-counter algorithms. Consistent with the results of a previous study (9), a high CD8 T-cell score was revealed to be associated with a better prognosis in patients with OC. Thereafter, 580 CD8 T cell-related genes were identified by comparing the gene expression profiles of the CD8 T cell high- and low-score groups. A PPI network was then constructed and the molecular mechanisms of the genes were explored by GO enrichment analysis. The results demonstrated that the majority of the hub genes were associated with 'T cell activation'. Subsequent survival analysis of the selected hub genes revealed that *STAT4* has a potential value as a predictive biomarker of survival and as an indicator of CD8 T-cell infiltration in OC. Furthermore, comprehensive assessment across multiple independent OC cohorts showed that the *STAT4* high-expression group had a significantly longer OS time compared with the low-expression group, which is consistent with the previous studies on cancer outcomes (14-16,42). In addition, Wubetu *et al* (43) revealed that STAT4 expression was positively correlated with CD8 T-cell infiltration in hepatocellular carcinoma tissues (43). Thus, *STAT4* may serve an important role in the recruitment of CD8 T-cell infiltration in OC.

A series of experiments and analyses were performed in the current study to obtain insights into the biological functions of *STAT4*. GO and KEGG analyses indicated that *STAT4* has a key role in the positive regulation of cytokine production and chemokine signaling pathways. Furthermore, *STAT4* and *CCL5* were highly correlated in multiple independent cohorts of OC. A previous study reported that loss of CCL5 resulted in a significant reduction of CD8 T-cell infiltration in human and murine ovarian cancer (21). Collectively, these

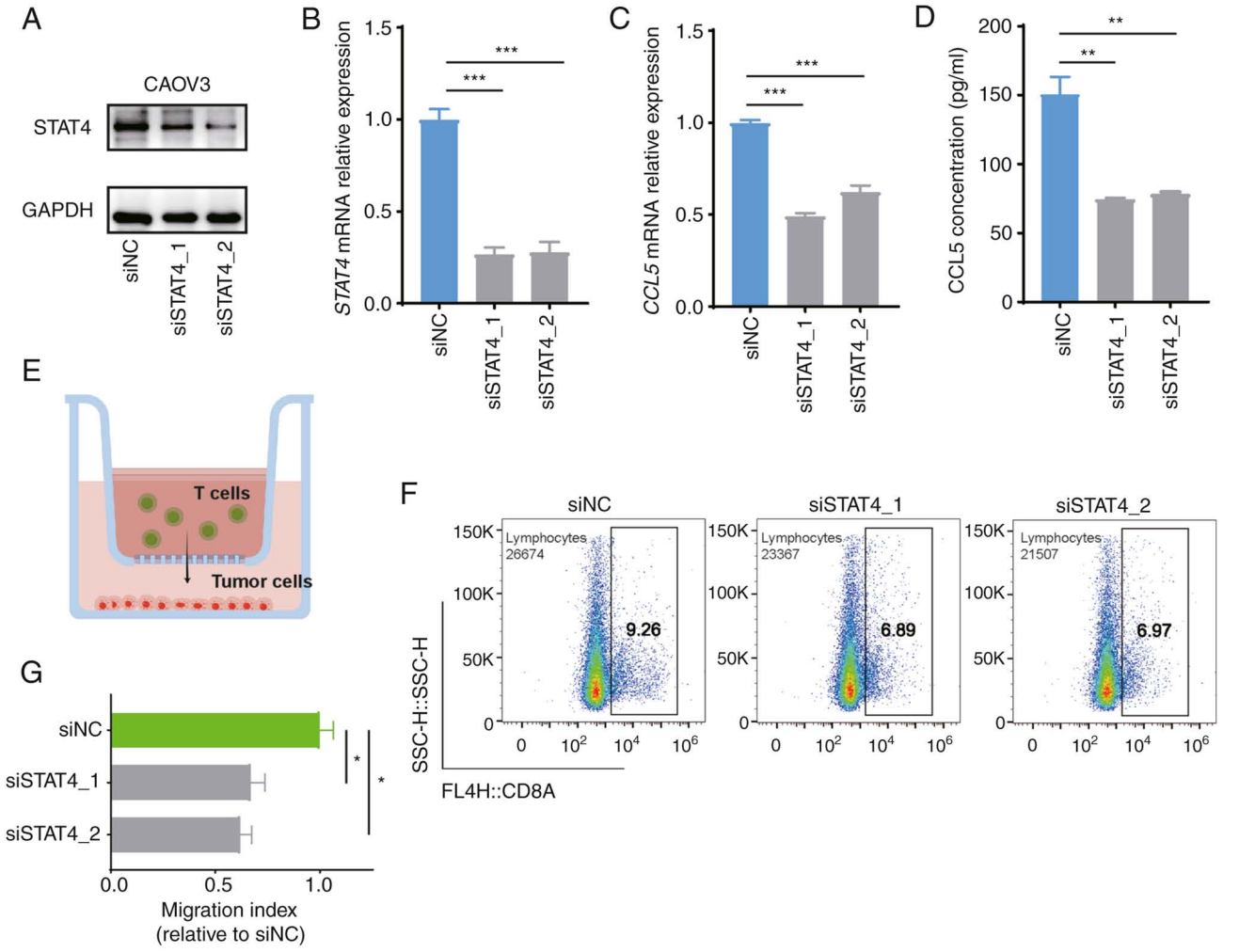

Figure 6. STAT4 induces CCL5 secretion and promotes CD8 T-cell migration. (A) Verification of STAT4 expression by western blotting in CAOV3 cells transfected with siRNA. GAPDH was used as a loading control. (B) Established cells were examined at the mRNA level. *STAT4* knockdown in CAOV3 cells led to reduced CCL5 at the (C) mRNA level and (D) in culture supernatants. (E) Diagram of the chemotaxis assay of autologous blood T cells toward supernatants derived from ovarian serous carcinoma cells. (F) Flow cytometric analysis of $CD8A^+$ cells in the bottom chamber. (G) Semi-quantification of $CD8A^+$ cells that migrated into the bottom chamber. $^*P<0.05$, $^{**}P\leq0.01$ and $^{***}P\leq0.001$, one-way ANOVA with Tukey's post hoc test. si, small interfering; NC, negative control; STAT4, signal transducer and activator of transcription 4; CCL5, CC chemokine ligand 5.

results suggested that *STAT4* may regulate CCL5 secretion to enhance CD8 T-cell infiltration. Furthermore, STAT4, CCL5 and CD8A levels were revealed to be significantly correlated in OC tissues at both mRNA and protein levels. In addition, *STAT4* knockdown in the CAOV3 cell line led to a corresponding reduction in CCL5 expression and CD8 T-cell migration. These results are consistent with a study by Dangaj *et al* (21), which suggested that tumor-derived CCL5 is a key contributor to the regulation of immune cell infiltration in ovarian cancer, resulting in an improved clinical benefit for patients. Additionally, Pasquier *et al* reported that ovarian cancer stromal cells can induce chemoresistance by secreting CCL5, thus promoting cancer progression (44). Moreover, CCL5 secretion by cancer-associated fibroblasts has been shown to promote the metastasis of hepatocellular carcinoma by activating the HIF1α/ZEB1 axis (45). These results indicated that CCL5 has different functions in different types of cancer.

The present study demonstrated that *STAT4* is an important positive regulator of CCL5 expression in OC. It has been demonstrated that DNA methylation can silence *CCL5* expression, which may be used as a potential mechanism for its negative regulation (46). Additionally, the WNT/β-catenin gene signature is specifically upregulated in low-CCL5 melanoma tumors (18). Notably, DNA methyltransferase 1 inhibition has been reported to increase the expression of the T-cell chemoattractant, CCL5, in lung cancer via suppression of MYC signaling (47). These pathways may interact with each other and affect the expression of CCL5, which can be explored further in future research.

In conclusion, the present study revealed that *STAT4* may be an independent factor for favorable prognosis in OC, with the high *STAT4*-expression group having a longer survival compared with the low *STAT4*-expression group, thus suggesting that *STAT4* may be a novel prognostic biomarker for OC. Furthermore, the present data indicated that *STAT4* acts as an important regulator of CD8 T-cell infiltration in OC tissues by regulating the secretion of CCL5. However, these experiments were performed *in vitro* and should be verified by *in vivo* studies in future research.

Acknowledgments

Not applicable.

Funding

This work was supported by the Nature and Science Foundation of China (grant nos. 81974408, 81874106, 82073259), the Key R&D Program of Hubei Province (grant no. 2020BCA067), the Hubei Province Science Fund for Distinguished Young Scholars (grant no. 2020CFA066) and the Beijing Kanghua Foundation for the Development of Traditional Chinese and Western Medicine (grant no. KH-2021-LQJJ-006).

Availability of data and materials

The datasets generated and/or analyzed during the current study are available in TCGA and GEO repositories (TCGA, https://portal.gdc.cancer.gov/repository; GSE130571, https://www.ncbi.nlm.nih.gov/geo/query/acc.cgi?acc=GSE130571; GSE53963, https://www.ncbi.nlm.nih.gov/geo/query/acc.cgi?acc=GSE53963;GSE32062,https://www.ncbi.nlm.nih.gov/geo/query/acc.cgi?acc=GSE32062). The remaining datasets used and/or analyzed during the current study are available from the corresponding author on reasonable request.

Authors' contributions

WW, GC and CYS conceived the study. WW and SL confirm the authenticity of all the raw data. WW performed the experiments. FNL collected clinical data and samples. SL, BY, XCZ and JJY performed data analysis. WW wrote the manuscript. SL, GC and CYS supervised and revised the paper. GC and CYS provided equipment and funding. All of the authors read and approved the final manuscript.

Ethics approval and consent to participate

The present study was approved by the Ethics Committee of Tongji Hospital (approval no. TJ-IRB20190320), and patients provided written informed consent.

Patient consent for publication

Written informed consent for publication was obtained from the patients.

Competing interests

The authors declare that they have no competing interests.

References

1. Siegel RL, Miller KD, Fuchs HE and Jemal A: Cancer statistics, 2022. CA Cancer J Clin 72: 7-33, 2022.
2. Dao F, Schlappe BA, Tseng J, Lester J, Nick AM, Lutgendorf SK, McMeekin S, Coleman RL, Moore KN, Karlan BY, *et al*: Characteristics of 10-year survivors of high-grade serous ovarian carcinoma. Gynecol Oncol 141: 260-263, 2016.
3. Torre LA, Trabert B, DeSantis CE, Miller KD, Samimi G, Runowicz CD, Gaudet MM, Jemal A and Siegel RL: Ovarian Cancer Statistics, 2018. CA Cancer J Clin 68: 284-296, 2018.
4. Garziera M, Cecchin E, Giorda G, Sorio R, Scalone S, De Mattia E, Roncato R, Gagno S, Poletto E, Romanato L, *et al*: Clonal evolution of TP53 c.375+1G > A mutation in pre- and post-neo-adjuvant chemotherapy (NACT) tumor samples in high-grade serous ovarian cancer (HGSOC). Cells 8: 1186, 2019.
5. Leary A, Tan D and Ledermann J: Immune checkpoint inhibitors in ovarian cancer: Where do we stand? Ther Adv Med Oncol 13: 17588359211039899, 2021.
6. Hamanishi J, Mandai M, Ikeda T, Minami M, Kawaguchi A, Murayama T, Kanai M, Mori Y, Matsumoto S, Chikuma S, *et al*: Safety and antitumor activity of Anti-PD-1 antibody, nivolumab, in patients with platinum-resistant ovarian cancer. J Clin Oncol 33: 4015-4022, 2015.
7. Ji RR, Chasalow SD, Wang L, Hamid O, Schmidt H, Cogswell J, Alaparthy S, Berman D, Jure-Kunkel M, Siemers NO, *et al*: An immune-active tumor microenvironment favors clinical response to ipilimumab. Cancer Immunol Immunother 61: 1019-1031, 2012.
8. Pautu JL and Kumar L: Intratumoral T cells and survival in epithelial ovarian cancer. Natl Med J India 16: 150-151, 2003.
9. Ovarian Tumor Tissue Analysis (OTTA) Consortium; Goode EL, Block MS, Kalli KR, Vierkant RA, Chen W, Fogarty ZC, Gentry-Maharaj A, Tołoczko A, Hein A, *et al*: Dose-Response association of CD8+ Tumor-Infiltrating lymphocytes and survival time in high-grade serous ovarian cancer. JAMA Oncol 3: e173290, 2017.
10. Kaplan MH: STAT4-A critical regulator of inflammation in vivo. Immunol Res 31: 231-241, 2005.
11. Thierfelder WE, Van Deursen JM, Yamamoto K, Tripp RA, Sarawar SR, Carson RT, Sangster MY, Vignali DA, Doherty PC, Grosveld GC and Ihle JN: Requirement for Stat4 in interleukin-12-mediated responses of natural killer and T cells. Nature 382: 171-174, 1996.
12. Kuroda E, Kito T and Yamashita U: Reduced expression of STAT4 and IFN-gamma in macrophages from BALB/c mice. J Immunol 168: 5477-5482, 2002.
13. Bacon CM, Petricoini EF III, Ortaldo JR, Rees RC, Larner AC, Johnston JA and O'Shea JJ: Interleukin 12 induces tyrosine phosphorylation and activation of STAT4 in human lymphocytes. Proc Natl Acad Sci USA 92: 7307-7311, 1995.
14. Wang G, Chen JH, Qiang Y, Wang DZ and Chen Z: Decreased STAT4 indicates poor prognosis and enhanced cell proliferation in hepatocellular carcinoma. World J Gastroenterol 21: 3983-3993, 2015.
15. Li S, Sheng B, Zhao M, Shen Q, Zhu H and Zhu X: The prognostic values of signal transducers activators of transcription family in ovarian cancer. Biosci Rep 37: BSR20170650, 2017.
16. Wang S, Yu L, Shi W, Li X and Yu L: Prognostic roles of signal transducers and activators of transcription family in human breast cancer. Biosci Rep 38: BSR20171175, 2018.
17. Harlin H, Meng Y, Peterson AC, Zha Y, Tretiakova M, Slingluff C, McKee M and Gajewski TF: Chemokine expression in melanoma metastases associated with CD8+ T-cell recruitment. Cancer Res 69: 3077-3085, 2009.
18. Spranger S, Bao R and Gajewski TF: Melanoma-intrinsic β-catenin signalling prevents anti-tumour immunity. Nature 523: 231-235, 2015.
19. Sanchez-Paulete AR, Cueto FJ, Martínez-López M, Labiano S, Morales-Kastresana A, Rodríguez-Ruiz ME, Jure-Kunkel M, Azpilikueta A, Aznar MA, Quetglas JI, *et al*: Cancer immunotherapy with immunomodulatory Anti-CD137 and Anti-PD-1 monoclonal antibodies requires BATF3-Dependent dendritic cells. Cancer Discov 6: 71-79, 2016.
20. Zsiros E, Duttagupta P, Dangaj D, Li H, Frank R, Garrabrant T, Hagemann IS, Levine BL, June CH, Zhang L, *et al*: The ovarian cancer chemokine landscape is conducive to homing of Vaccine-Primed and CD3/CD28-Costimulated T cells prepared for adoptive therapy. Clin Cancer Res 21: 2840-2850, 2015.
21. Dangaj D, Bruand M, Grimm AJ, Ronet C, Barras D, Duttagupta PA, Lanitis E, Duraiswamy J, Tanyi JL, Benencia F, *et al*: Cooperation between constitutive and inducible chemokines enables T cell engraftment and immune attack in solid tumors. Cancer Cell 35: 885-900.e10, 2019.
22. Liu J, Lichtenberg T, Hoadley KA, Poisson LM, Lazar AJ, Cherniack AD, Kovatich AJ, Benz CC, Levine DA, Lee AV, *et al*: An Integrated TCGA Pan-cancer clinical data resource to drive High-Quality survival outcome analytics. Cell 173: 400-416.e11, 2018.

23. Konecny GE, Wang C, Hamidi H, Winterhoff B, Kalli KR, Dering J, Ginther C, Chen HW, Dowdy S, Cliby W, *et al*: Prognostic and therapeutic relevance of molecular subtypes in high-grade serous ovarian cancer. J Natl Cancer Inst 106: dju249, 2014.
24. Yoshihara K, Tsunoda T, Shigemizu D, Fujiwara H, Hatae M, Fujiwara H, Masuzaki H, Katabuchi H, Kawakami Y, Okamoto A, *et al*: High-Risk ovarian cancer based on 126-Gene expression signature is uniquely characterized by downregulation of antigen presentation pathway. Clin Cancer Res 18: 1374-1385, 2012.
25. Ramaswamy V, Remke M, Bouffet E, Faria CC, Perreault S, Cho YJ, Shih DJ, Luu B, Dubuc AM, Northcott PA, *et al*: Recurrence patterns across medulloblastoma subgroups: An integrated clinical and molecular analysis. Lancet Oncol 14: 1200-1207, 2013.
26. Hill RM, Kuijper S, Lindsey JC, Petrie K, Schwalbe EC, Barker K, Boult JK, Williamson D, Ahmad Z, Hallsworth A, *et al*: Combined MYC and P53 defects emerge at medulloblastoma relapse and define rapidly progressive, therapeutically targetable disease. Cancer Cell 27: 72-84, 2015.
27. Sun Y, Wu L, Zhong Y, Hou Y, Wang Z, Zhang Z, Xie J, Wang C, Chen D, Huang Y, *et al*: Single-cell landscape of the ecosystem in early-relapse hepatocellular carcinoma. Cell 184: 404-421.e16, 2021.
28. Becht E, Giraldo NA, Lacroix L, Buttard B, Elarouci N, Petitprez F, Selves J, Laurent-Puig P, Sautès-Fridman C, Fridman WH and de Reyniès A: Estimating the population abundance of tissue-infiltrating immune and stromal cell populations using gene expression. Genome Biol 17: 218, 2016.
29. Finotello F, Mayer C, Plattner C, Laschober G, Rieder D, Hackl H, Krogsdam A, Loncova Z, Posch W, Wilflingseder D, *et al*: Molecular and pharmacological modulators of the tumor immune contexture revealed by deconvolution of RNA-seq data. Genome Med 11: 34, 2019.
30. Szklarczyk D, Gable AL, Lyon D, Junge A, Wyder S, Huerta-Cepas J, Simonovic M, Doncheva NT, Morris JH, Bork P, *et al*: STRING v11: Protein-protein association networks with increased coverage, supporting functional discovery in genome-wide experimental datasets. Nucleic Acids Res 47: D607-D613, 2019.
31. Yu G, Wang LG, Han Y and He QY: clusterProfiler: An R package for comparing biological themes among gene clusters. OMICS 16: 284-287, 2012.
32. Azim HA Jr, Peccatori FA, Brohée S, Branstetter D, Loi S, Viale G, Piccart M, Dougall WC, Pruneri G and Sotiriou C: RANK-ligand (RANKL) expression in young breast cancer patients and during pregnancy. Breast Cancer Res 17: 24, 2015.
33. Livak KJ and Schmittgen TD: Analysis of relative gene expression data using real-time quantitative PCR and the 2(T)(-Delta Delta C) method. Methods 25: 402-408, 2001.
34. Ling S, Pang J, Yu J, Wang R, Liu L, Ma Y, Zhang Y, Jin N and Wang S: Preparation and identification of monoclonal antibody against fumonisin B-(1) and development of detection by Ic-ELISA. Toxicon 80: 64-72, 2014.
35. Jones CC, Mercaldo SF, Blume JD, Wenzlaff AS, Schwartz AG, Chen H, Deppen SA, Bush WS, Crawford DC, Chanock SJ, *et al*: Racial disparities in lung cancer survival: The contribution of stage, treatment, and ancestry. J Thorac Oncol 13: 1464-1473, 2018.
36. Ju YJ, Lee SW, Kye YC, Lee GW, Kim HO, Yun CH and Cho JH: Self-reactivity controls functional diversity of naive $CD8^+$ T cells by co-opting tonic type I interferon. Nat Commun 12: 6059, 2021.
37. Burgueno-Bucio E, Mier-Aguilar CA and Soldevila G: The multiple faces of CD5. J Leukoc Biol 105: 891-904, 2019.
38. Gordiienko I, Shlapatska L, Kovalevska L and Sidorenko SP: SLAMF1/CD150 in hematologic malignancies: Silent marker or active player? Clin Immunol 204: 14-22, 2019.
39. Yang C, Mai H, Peng J, Zhou B, Hou J and Jiang D: STAT4: An immunoregulator contributing to diverse human diseases. Int J Biol Sci 16: 1575-1585, 2020.
40. Yatim N, Cullen S and Albert ML: Dying cells actively regulate adaptive immune responses. Nat Rev Immunol 17: 262-275, 2017.
41. Sturm G, Finotello F, Petitprez F, Zhang JD, Baumbach J, Fridman WH, List M and Aneichyk T: Comprehensive evaluation of transcriptome-based cell-type quantification methods for immuno-oncology. Bioinformatics 35: i436-i445, 2019.
42. Nishi M, Batsaikhan BE, Yoshikawa K, Higashijima J, Tokunaga T, Takasu C, Kashihara H, Ishikawa D and Shimada M: High STAT4 expression indicates better disease-free survival in patients with gastric cancer. Anticancer Res 37: 6723-6729, 2017.
43. Wubetu GY, Utsunomiya T, Ishikawa D, Yamada S, Ikemoto T, Morine Y, Iwahashi S, Saito Y, Arakawa Y, Imura S, *et al*: High STAT4 expression is a better prognostic indicator in patients with hepatocellular carcinoma after hepatectomy. Ann Surg Oncol 21 (Suppl 4): S721-S728, 2014.
44. Pasquier J, Gosset M, Geyl C, Hoarau-Véchot J, Chevrot A, Pocard M, Mirshahi M, Lis R, Rafii A and Touboul C: CCL2/CCL5 secreted by the stroma induce IL-6/PYK2 dependent chemoresistance in ovarian cancer. Mol Cancer 17: 47, 2018.
45. Xu H, Zhao J, Li J, Zhu Z, Cui Z, Liu R, Lu R, Yao Z and Xu Q: Cancer associated fibroblast-derived CCL5 promotes hepatocellular carcinoma metastasis through activating HIF1 α/ZEB1 axis. Cell Death Dis 13: 478, 2022.
46. Li H, Chiappinelli KB, Guzzetta AA, Easwaran H, Yen RW, Vatapalli R, Topper MJ, Luo J, Connolly RM, Azad NS, *et al*: Immune regulation by low doses of the DNA methyltransferase inhibitor 5-azacitidine in common human epithelial cancers. Oncotarget 5: 587-598, 2014.
47. Topper MJ, Vaz M, Chiappinelli KB, DeStefano Shields CE, Niknafs N, Yen RC, Wenzel A, Hicks J, Ballew M, Stone M, *et al*: Epigenetic therapy Ties MYC depletion to reversing immune evasion and treating lung cancer. Cell 171: 1284-1300.e21, 2017.